A numerical integrator for the two-fixed-centres problem conserving all constants of motion

2006 J. Phys. A: Math. Gen. 39 9437

(http://iopscience.iop.org/0305-4470/39/30/004)

INSTITUTE OF PHYSICS PUBLISHING JOURNAL OF PHYSICS A: MATHEMATICAL AND GENERAL

J. Phys. A: Math. Gen. **39** (2006) 9437–9452 doi:10.1088/0305-4470/39/30/004

A numerical integrator for the two-fixed-centres problem conserving all constants of motion

Tsuyoshi Inoue and Yukitaka Minesaki

Department of Applied Mathematics and Physics, Graduate School of Informatics, Kyoto University, Kyoto 606-8501, Japan

E-mail: minesaki@i.kyoto-u.ac.jp

Received 1 February 2006
Published 12 July 2006
Online at stacks.iop.org/JPhysA/39/9437

Abstract

The two-fixed-centres problem describes the motion of a particle influenced by the gravitational pull of two fixed particles. This is a well-known integrable Hamiltonian system having three constants of motion. This paper presents a discrete two-dimensional two-fixed-centres problem which conserves two of these constants of motion. Moreover, this discrete system preserves the discrete analogue of the third constant of motion. A canonical transformation is introduced to separate the variables and remove singularities of the system. A combination of this transformation and energy-preserving method plays an important role in deriving the discrete system with a variable time step.

PACS numbers: 02.60.Jh, 02.70.Bf, 45.10.−b, 91.10.Sp

1. Introduction

To numerically solve a differential system, we must build a discrete model corresponding to the original system. This process is called a discretization, among which Euler's method and the Runge–Kutta method are common. Generally, a discrete system given by a discretization describes a system different from the original system. Global characteristics of the original system, for example, existence of constants of motion, monotonicity, or boundedness, generally disappear through discretization.

Geometric integrators concentrate on these qualitative properties, and they conserve one or more of them exactly (up to round-off error). A number of books [6, 9] and review papers [10, 11] have been written on the subject, and the recent advancements in this field are remarkable. Symplectic integrators for Hamiltonian systems, symmetric integrators for reversible systems and methods preserving energies or first integrals are well-known examples of geometric integrators.

Symplectic integrators [6, 9, 20] are commonly used to simulate Hamiltonian systems numerically. They conserve a global characteristic called the symplectic structure. As a result,

these integrators have a constant of motion $\tilde{H} = H + \delta H_1 + \delta^2 H_2 + \cdots$ where δ is a time step. $\tilde{H}$ is a discrete analogue of the Hamiltonian H. Moreover, symplectic integrators keep the value of a discrete momentum derived through a discrete Noether's theorem [19]. Because of this characteristic, symplectic integrators tend to be numerically stable in the long-time simulation.

Minesaki and Nakamura [12, 13] present discretizations of the Kepler problem which conserve all constants of motion including the Runge–Lenz vectors. They also give a discretization for the Stäckel system which conserves all constants of motion [14]. The Stäckel system is a class of separable Hamiltonian systems including the Kepler problem. The discretization consists of separation of variables and the energy-preserving method [3, 4].

The two-fixed-centres problem (2FCP) expresses the motion of a particle affected by gravitational pull of two fixed particles. The 2FCP is a separable Hamiltonian system, and an instance of the Stäckel system. Since the two-dimensional 2FCP has two constants of motion, it is integrable in the sense of Liouville–Arnold. It was in 18th century when the analytical expression of the solution was obtained by Euler. After that the 2FCP has been studied as an important example of integrable dynamical systems [1, 18]. Varvoglis *et al* present a canonical transformation that removes singularities of the canonical equation of the separated 2FCP [18].

The 2FCP is regarded as an addition of an integrable perturbation to the Kepler motion [2]. It describes a wider range of motion including the Kepler motion. A discretization of the 2FCP which conserves its global characteristics will be a step to construct better discretizations for more complicated dynamical systems such as the three-body problem.

In this paper we separate the variables of the two-dimensional 2FCP and remove its singularities following the work of Varvoglis [18]. Then the discretization method presented by Minesaki–Nakamura [14] is applied to obtain the discrete system. The discrete system has the same two constants of motion as those of the original 2FCP. Furthermore, the discrete system has an additional constant of motion. This is shown to be a discrete analogue of the continuous system's third constant of motion which has an integral form. Then we conduct numerical experiments and observe that the discrete system remarkably approximates the trajectory of the continuous system.

The paper is organized as follows. In section 2, separation of variables and removal of singularities are done according to Varvoglis [18]. In section 3, the energy-preserving method [3, 4] is applied to each term of the Hamiltonian of the separated system. As a result, the discrete system has two constants of motion. In section 4, we discuss the constants of motion of the discrete system in detail. In section 5, we argue a global characteristic which the discrete system retains through discretization. This results from the existence of the two constants of motion which have the same form as those of the continuous system. In section 6, we confirm the effect of our discretization by a numerical experiment. Then we compare the discrete system with a symplectic integrator.

2. Separation of variables of 2FCP

We begin with the 2FCP [15] defined by the Hamiltonian

$$H_c(x, y, p_x, p_y) = \frac{p_x^2}{2} + \frac{p_y^2}{2} - \frac{\alpha_1}{r_1} - \frac{\alpha_2}{r_2} - h_c, \tag{1}$$

where $r_1 = \sqrt{(x+1)^2 + y^2}$ and $r_2 = \sqrt{(x-1)^2 + y^2}$. The fixed particles are at $(-1, 0)$ and $(1, 0)$. We fix the value of constant h_c so that

$$H_c(x, y, p_x, p_y) \equiv 0. \tag{2}$$

Here (x, y) is the location of the moving particle with unit mass, and p_x and p_y are conjugate momenta. The constants α_1 and α_2 are expressed as $\alpha_1 = 2\mu$ and $\alpha_2 = 2(1-\mu)$, $\mu \in [0, 1]$, where the parameter μ denotes the mass ratio of the two fixed particles.

The 2FCP (1) is a separable Hamiltonian system [15] which can be integrated by using the elliptic coordinates

$$\xi = \frac{r_1 + r_2}{2}, \qquad \eta = \frac{r_1 - r_2}{2}. \tag{3}$$

In the elliptic coordinates (ξ, η) and the corresponding canonical momenta p_ξ, p_η, the original canonical variables x, y, p_x, p_y are written as

$$\begin{aligned} x &= \xi\eta, \quad y = (\operatorname{sign} y)\sqrt{(\xi^2-1)(1-\eta^2)}, \\ p_x &= \frac{\eta(\xi^2-1)p_\xi + \xi(1-\eta^2)p_\eta}{\xi^2-\eta^2}, \\ p_y &= (\operatorname{sign} y)\sqrt{(\xi^2-1)(1-\eta^2)}\frac{(\xi p_\xi - \eta p_\eta)}{\xi^2-\eta^2}, \end{aligned} \tag{4}$$

where $(\operatorname{sign} y)$ is the sign of y. Through the canonical transformation (4), the original Hamiltonian (1) leads to the Hamiltonian

$$H_e(\xi, \eta, p_\xi, p_\eta) = \frac{K_\xi(\xi, p_\xi) + K_\eta(\eta, p_\eta)}{\xi^2-\eta^2} \equiv 0, \tag{5}$$

where $K_\xi(\xi, p_\xi)$ and $K_\eta(\eta, p_\eta)$ are

$$\begin{aligned} K_\xi(\xi, p_\xi) &\stackrel{\text{def}}{=} \tfrac{1}{2}(\xi^2-1)p_\xi^2 + \alpha\xi - h_c\xi^2, \\ K_\eta(\eta, p_\eta) &\stackrel{\text{def}}{=} \tfrac{1}{2}(1-\eta^2)p_\eta^2 + \beta\eta + h_c\eta^2, \end{aligned} \tag{6}$$

respectively. Here we set the constants $\alpha = -\alpha_1 - \alpha_2$ and $\beta = \alpha_1 - \alpha_2$.

We can regard the time variable t as a new canonical coordinate, so $-h_c$ conjugates to t in an extended phase space (cf [17]). We introduce a canonical transformation

$$\{p_\xi, p_\eta, -h_c, \xi, \eta, t\} \to \{p_\xi, p_\eta, -k_c, \xi, \eta, s\}$$

such that

$$h_c \to k_c, \qquad k_c = (\xi^2-\eta^2)h_c, \qquad t \to s, \qquad \mathrm{d}s = \frac{\mathrm{d}t}{\xi^2-\eta^2}. \tag{7}$$

The original Hamiltonian system with the Hamiltonian (1) is changed to

$$\frac{\mathrm{d}p_\xi}{\mathrm{d}s} = -\xi p_\xi^2 - \alpha + 2h_c\xi, \qquad \frac{\mathrm{d}\xi}{\mathrm{d}s} = (\xi^2-1)p_\xi, \tag{8}$$

$$\frac{\mathrm{d}p_\eta}{\mathrm{d}s} = \eta p_\eta^2 - \beta - 2h_c\eta, \qquad \frac{\mathrm{d}\eta}{\mathrm{d}s} = (1-\eta^2)p_\eta. \tag{9}$$

Now the Hamiltonian system (8), (9) is separated. Each set of equations (8), (9) is considered as the canonical equations given by the Hamiltonians K_ξ and K_η, respectively. Then K_ξ, K_η are the constants of motion of the 2FCP.

Although a discretization is necessary to solve equations (8), (9) numerically, the behaviour of the resulting discrete system is sometimes different from that of the original Hamiltonian system because of possible overflow near singularities. The overflow occurs near $\xi = 1$ and $\eta = \pm 1$ where the moving particle crosses the line connecting the two fixed particles. This makes it difficult to compute the 2FCP with high accuracy.

The Hamiltonian system (8), (9) gives the relationship

$$p_\xi = \frac{1}{\xi^2 - 1}\frac{\mathrm{d}\xi}{\mathrm{d}s}, \qquad p_\eta = \frac{1}{1 - \eta^2}\frac{\mathrm{d}\eta}{\mathrm{d}s}, \tag{10}$$

which suggests that the neighbourhood of $\xi = 1$ and that of $\eta = \pm 1$, where the overflow occurs, are around the singularities of p_ξ and p_η. Therefore, numerical simulation becomes inaccurate when the particle comes around the singularities of p_ξ and p_η.

In order to remove such singularities, we introduce the following canonical transformations $(\xi, \eta, p_\xi, p_\eta) \to (u, v, p_u, p_v)$ following the study of Varvoglis and Vozikis [18],

$$\xi = \cosh u, \quad \eta = \cos v, \qquad p_\xi = \frac{p_u}{\sinh u}, \qquad p_\eta = -\frac{p_v}{\sin v}. \tag{11}$$

Then the separated Hamiltonians K_ξ and K_η lead to

$$K_u(u, p_u) \overset{\text{def}}{=} K_\xi(\xi(u), p_\xi(u, p_u)) = \tfrac{1}{2}p_u^2 + \alpha\cosh u - h_c\cosh^2 u, \tag{12}$$

$$K_v(v, p_v) \overset{\text{def}}{=} K_\eta(\eta(v), p_\eta(v, p_v)) = \tfrac{1}{2}p_v^2 + \beta\cos v + h_c\cos^2 v. \tag{13}$$

As a result, the Hamiltonian system (8), (9) reduces to

$$\frac{\mathrm{d}u}{\mathrm{d}s} = p_u, \qquad \frac{\mathrm{d}p_u}{\mathrm{d}s} = -\alpha\sinh u + 2h_c\cosh u\sinh u, \tag{14}$$

$$\frac{\mathrm{d}v}{\mathrm{d}s} = p_v, \qquad \frac{\mathrm{d}p_v}{\mathrm{d}s} = \beta\sin v + 2h_c\cos v\sin v. \tag{15}$$

Each set of equations (14) and (15) can be regarded as the Hamiltonian systems given by K_u and K_v, respectively. The singularities in the elliptic coordinate system $(\xi, \eta, p_\xi, p_\eta)$ are removed in (14) and (15). The canonical transformation (x, y, p_x, p_y) to (u, v, p_u, p_v) is expressed as a composition of two canonical transformations (4) and (11), that is

$$\begin{aligned} u &= \cosh^{-1}\xi, \qquad v = \begin{cases} \cos^{-1}\eta, & y \geqslant 0, \\ 2\pi - \cos^{-1}\eta, & y < 0, \end{cases} \\ p_u &= p_x\sinh u\cos v + p_y\cosh u\sin v, \\ p_v &= -p_x\cosh u\sin v + p_y\sinh u\cos v. \end{aligned} \tag{16}$$

The inverse transformation of (16) is as follows:

$$\begin{aligned} x &= \cosh u\cos v, \quad y = \sinh u\sin v, \\ p_x &= \frac{p_u\cos v\sinh u - p_v\cosh u\sin v}{\cosh^2 u - \cos^2 v}, \\ p_y &= \frac{p_u\sin v\cosh u + p_v\sinh u\sin v}{\cosh^2 u - \cos^2 v}. \end{aligned} \tag{17}$$

3. Discrete two-fixed-centres problem

In the previous section, we have reduced 2FCP to two one-degree-of-freedom Hamiltonian systems through the canonical transformation (7). One is the Hamiltonian system (14) with the Hamiltonian K_u and the time variable s. The other is the Hamiltonian system (15) with the Hamiltonian K_v and the time variable s.

We apply the energy-preserving method [3, 4, 7] to the Hamiltonian system (14), (15). The following discrete system results:

$$\begin{aligned}
&\Delta_{+s}u^{(j)} = \frac{1}{2}\bigl(p_u^{(j+1)} + p_u^{(j)}\bigr),\\
&\Delta_{+s}p_u^{(j)} = (h_c(\cosh u^{(j+1)} + \cosh u^{(j)}) - \alpha)\frac{\cosh u^{(j+1)} - \cosh u^{(j)}}{u^{(j+1)} - u^{(j)}},\\
&s^{(0)} < s^{(1)} < \cdots, \qquad j = 0, 1, 2, \ldots,
\end{aligned} \tag{18}$$

where $u^{(j)}$ and $p_u^{(j)}$ are the values of discrete canonical variables at the discrete time $s^{(j)}$. A forward difference operator Δ_{+s} acting on a function $f\bigl(x_1^{(j)}, x_2^{(j)}, \ldots, x_m^{(j)}\bigr)$ is defined as follows:

$$\Delta_{+s} f\bigl(x_1^{(j)}, x_2^{(j)}, \ldots, x_m^{(j)}\bigr) \stackrel{\text{def}}{=} \frac{f\bigl(x_1^{(j+1)}, x_2^{(j+1)}, \ldots, x_m^{(j+1)}\bigr) - f\bigl(x_1^{(j)}, x_2^{(j)}, \ldots, x_m^{(j)}\bigr)}{s^{(j+1)} - s^{(j)}}. \tag{19}$$

Here $x_1^{(j)}, x_2^{(j)}, \ldots, x_m^{(j)}$, are functions of the discrete time $s^{(j)}$ The discrete system (18) conserves the Hamiltonian K_u. It converges to the continuous canonical equations (14) at the limit of $s^{(j+1)} - s^{(j)} \to 0$, $j = 0, 1, 2, \ldots$. Note that this method allows a variable step size.

Similarly, the Hamiltonian system (15) with the Hamiltonian K_v can be discretized with the energy-preserving method. By introducing discrete canonical variables $v^{(j)}$, $p_v^{(j)}$, $j = 0, 1, 2, \ldots$, we get the discrete Hamiltonian system

$$\begin{aligned}
&\Delta_{+s}v^{(j)} = \frac{1}{2}\bigl(p_v^{(j+1)} + p_v^{(j)}\bigr),\\
&\Delta_{+s}p_v^{(j)} = -(h_c(\cos v^{(j+1)} + \cos v^{(j)}) + \beta)\frac{\cos v^{(j+1)} - \cos v^{(j)}}{v^{(j+1)} - v^{(j)}},\\
&s^{(0)} < s^{(1)} < \cdots, \qquad j = 0, 1, 2, \ldots.
\end{aligned} \tag{20}$$

This discrete system has K_v as a constant of motion. It converges to the Hamiltonian system (15) at the limit of $s^{(j+1)} - s^{(j)} \to 0$.

We define a new discrete time variable $t^{(j)}$ by

$$t^{(j+1)} - t^{(j)} \equiv (\cosh^2 u^{(j)} - \cos^2 v^{(j)})(s^{(j+1)} - s^{(j)}), \qquad j = 0, 1, 2, \ldots. \tag{21}$$

As $\cosh u^{(j)} \geqslant 1$ and $-1 \leqslant \cos v^{(j)} \leqslant 1$, the discrete time $t^{(j)}$ satisfies $t^{(0)} \leqslant t^{(1)} \leqslant t^{(2)} \leqslant \cdots$. The relationship (21) is a discrete analogue of the time transformation $\mathrm{d}t = (\xi^2 - \eta^2)\,\mathrm{d}s$ which is used to separate the variables of the 2FCP with continuous time variable. Through (21) the discrete system (18) is transformed into

$$\begin{aligned}
&\Delta_{+t}u^{(j)} = \frac{1}{2}\frac{p_u^{(j+1)} + p_u^{(j)}}{\cosh^2 u^{(j)} - \cos^2 v^{(j)}},\\
&\Delta_{+t}p_u^{(j)} = \frac{h_c(\cosh u^{(j+1)} + \cosh u^{(j)}) - \alpha}{\cosh^2 u^{(j)} - \cos^2 v^{(j)}} \times \frac{\cosh u^{(j+1)} - \cosh u^{(j)}}{u^{(j+1)} - u^{(j)}},\\
&t^{(0)} \leqslant t^{(1)} \leqslant \cdots, \qquad j = 0, 1, 2, \ldots.
\end{aligned} \tag{22}$$

Similarly, the discrete system (20) is transformed into

$$\begin{aligned}
&\Delta_{+t}v^{(j)} = \frac{1}{2}\frac{p_v^{(j+1)} + p_v^{(j)}}{\cosh^2 u^{(j)} - \cos^2 v^{(j)}},\\
&\Delta_{+t}p_v^{(j)} = -\frac{h_c(\cos v^{(j+1)} + \cos v^{(j)}) + \beta}{\cosh^2 u^{(j)} - \cos^2 v^{(j)}} \times \frac{\cos v^{(j+1)} - \cos v^{(j)}}{v^{(j+1)} - v^{(j)}},\\
&t^{(0)} \leqslant t^{(1)} \leqslant \cdots, \qquad j = 0, 1, 2, \ldots.
\end{aligned} \tag{23}$$

We also define discrete canonical variables $x^{(j)}$, $y^{(j)}$, $p_x^{(j)}$ and $p_y^{(j)}$ derived from the discrete canonical variables $u^{(j)}$, $v^{(j)}$, $p_u^{(j)}$ and $p_v^{(j)}$ through (17). This is a discrete analogue of the canonical variables $x(t^{(j)})$, $y(t^{(j)})$, $p_x(t^{(j)})$ and $p_y(t^{(j)})$ at the discrete time $t^{(j)}$.

When an initial condition $(x^{(0)}, y^{(0)}, p_x^{(0)}, p_y^{(0)})$ is given, we can compute $\left(u^{(0)}, v^{(0)}, p_u^{(0)}, p_v^{(0)}\right)$ from the transformation (16). After determining the values of $u^{(j+1)}$, $v^{(j+1)}$, $p_u^{(j+1)}$ and $p_v^{(j+1)}$ by the discrete systems (22) and (23), we can derive the values of $x^{(j+1)}$, $y^{(j+1)}$, $p_x^{(j+1)}$ and $p_y^{(j+1)}$ through the canonical transformation (17). Therefore, the system (22), (23) turns out to be a discrete analogue of the 2FCP. We name the discrete system (22), (23) the *discrete* 2*FCP*. The discrete 2FCP is a first-order scheme; the energy-preserving method [3, 7] applied to the separated system (18) and (20) is of second order, while the discrete time-variable transformation (21) is a first-order approximation.

Note that the set of discrete equations (22) and (23) is an implicit numerical scheme. They do not, therefore, form one-to-one maps from $t^{(j)}$ to $t^{(j+1)}$. In order to solve the implicit scheme (22) and (23), we need a relaxation method. The computational cost of solving (22) and (23) is determined by the number of iterations of the relaxation method, which depends on how to set an initial guess for a relaxation method. In the numerical experiment of this paper, we use the following method to calculate the values $u^{(j+1)}$, $v^{(j+1)}$, $p_u^{(j+1)}$, $p_v^{(j+1)}$ at $s^{(j+1)}$, $j = 0, 1, 2, \ldots$. First, we compute approximate values of $u^{(j+1)}$, $v^{(j+1)}$, $p_u^{(j+1)}$, $p_v^{(j+1)}$ by using the Euler approximation of the Hamiltonian system (14), (15). Then we set these approximate values as initial values and calculate $u^{(j+1)}$, $v^{(j+1)}$, $p_u^{(j+1)}$, $p_v^{(j+1)}$ so as to satisfy (18) and (20) by using a relaxation method, such as Newton's method.

By using higher order energy-preserving methods (e.g., see [8]), implicit higher order discrete 2FCPs are obtained. However, we do not argue higher order discrete 2FCPs in this paper because the order does not affect qualitative behaviour of the discrete 2FCP, which will be discussed in sections 4 and 5.

4. Constants of motion

The 2FCP with the Hamiltonian (1) has the following two constants of motion [15].

(i) Hamiltonian in (1)

$$H_c(x, y, p_x, p_y) = \frac{p_x^2}{2} + \frac{p_y^2}{2} - \frac{\alpha_1}{r_1} - \frac{\alpha_2}{r_2} - h_c. \tag{24}$$

(ii) A constant of motion

$$I(x, y, p_x, p_y) = \frac{1}{2}(yp_x - xp_y)^2 + \frac{p_x^2}{2} + x\left(\frac{\alpha_1}{r_1} - \frac{\alpha_2}{r_2}\right). \tag{25}$$

These constants are expressed by u, v, p_u, p_v as follows:

$$H_c(x, y, p_x, p_y) = \left[\frac{K_u(u, p_u) + K_v(v, p_v)}{\cosh^2 u - \cos^2 v}\right]_{\substack{u = u(x,y),\ p_u = p_u(x,y,p_x,p_y),\\ v = v(x,y),\ p_v = p_v(x,y,p_x,p_y)}}, \tag{26}$$

$$\begin{aligned} I(x, y, p_x, p_y) &= -[K_u(u, p_u)]_{u=u(x,y),\, p_u=p_u(x,y,p_x,p_y)} \\ &= [K_v(v, p_v)]_{v=v(x,y),\, p_v=p_v(x,y,p_x,p_y)}. \end{aligned} \tag{27}$$

Therefore, the conservation of H_c and I in Cartesian coordinates (x, y, p_x, p_y) is equivalent to that of K_u and K_v in the separated coordinates (u, v, p_u, p_v) along with the condition $K_u + K_v = 0$. Since the 2FCP is a Hamiltonian system with two degrees of freedom having

two involutive integrals of motion, the system is integrable in the sense of Liouville–Arnold. The third constant of motion, which uniquely determines a trajectory in the four-dimensional phase space, can be obtained by quadrature.

Let us get the third constant J of motion in the coordinate system (u, v, p_u, p_v). By choosing two involutive constants of motion $K_u + K_v$ and K_u, the following canonical transformation can be formed:

$$\begin{pmatrix} u & v \\ p_u & p_v \end{pmatrix} \to \begin{pmatrix} s - s_0 & J \\ K_u + K_v & K_u \end{pmatrix}. \tag{28}$$

After the transformation (28), $K_u + K_v$ and K_u correspond to canonical momenta, where s is the time variable and s_0, J are constants. The constant J is the third constant of motion, and is written as

$$J(u, v, p_u, p_v) = \int \frac{\frac{\partial(K_u+K_v)}{\partial p_v}\,\mathrm{d}u - \frac{\partial(K_u+K_v)}{\partial p_u}\,\mathrm{d}v}{\frac{\partial((K_u+K_v),K_u)}{\partial(p_u,p_v)}}, \tag{29}$$

where

$$\frac{\partial(K_u + K_v, K_u)}{\partial(p_u, p_v)} \stackrel{\text{def}}{=} \det\begin{pmatrix} \frac{\partial(K_u+K_v)}{\partial p_u} & \frac{\partial K_u}{\partial p_u} \\ \frac{\partial(K_u+K_v)}{\partial p_v} & \frac{\partial K_u}{\partial p_v} \end{pmatrix}. \tag{30}$$

By calculating (30), the constant J leads to

$$J(u, v, p_u, p_v) = \int \frac{\mathrm{d}u}{p_u} - \int \frac{\mathrm{d}v}{p_v}. \tag{31}$$

From the definition of K_u, K_v, p_u and p_v are rewritten by u and v as

$$p_u^2 = 2(K_u - \alpha\cosh u + h_c\cosh^2 u), \tag{32}$$

$$p_v^2 = 2(K_v - \beta\cos v - h_c\cos^2 v). \tag{33}$$

Then each term in $J(u, v, p_u, p_v)$ is an indefinite integral with respect to u or v, respectively. However, the result of the integration is a multivalued function. Unlike other integrals H_c and I, J does not have an explicit form.

In the case of the discrete 2FCP (22) and (23), an argument about the constants of motion parallels the continuous case. As the discrete equations (22) and (23) are derived by the energy-preserving method, they clearly conserve two constants of motion $K_u\big(u^{(j)}, p_u^{(j)}\big)$ and $K_v\big(v^{(j)}, p_v^{(j)}\big)$ for $j = 0, 1, 2, \ldots$. Because of this conservation and the relationship (27), the discrete 2FCP (22), (23) preserves the following constants of motion.

(i) A discrete analogue of Hamiltonian

$$H_{\mathrm{d-c}}^{(j)} = H_c\big(x^{(j)}, y^{(j)}, p_x^{(j)}, p_y^{(j)}\big). \tag{34}$$

(ii) A discrete analogue of the constant of motion I

$$I_{\mathrm{d}}^{(j)} = I\big(x^{(j)}, y^{(j)}, p_x^{(j)}, p_y^{(j)}\big). \tag{35}$$

Moreover, the discrete 2FCP (22), (23) keeps the value of

$$J_{\mathrm{d}}^{(j)} \stackrel{\text{def}}{=} \sum_{i=0}^{j}\left(\frac{u^{(i+1)} - u^{(i)}}{\frac{1}{2}\big(p_u^{(i+1)} + p_u^{(i)}\big)} - \frac{v^{(i+1)} - v^{(i)}}{\frac{1}{2}\big(p_v^{(i+1)} + p_v^{(i)}\big)}\right), \qquad j = 0, 1, 2, \ldots. \tag{36}$$

Actually, the difference of $J_{\mathrm{d}}^{(j)}$ leads to

$$J_{\mathrm{d}}^{(j)} - J_{\mathrm{d}}^{(j-1)} = \left(\frac{\Delta_{+s} u^{(j)}}{\frac{1}{2}\left(p_u^{(j+1)} + p_u^{(j)}\right)} - \frac{\Delta_{+s} v^{(j)}}{\frac{1}{2}\left(p_v^{(j+1)} + p_v^{(j)}\right)} \right) (s^{(j+1)} - s^{(j)}) = 0 \tag{37}$$

by applying the discrete 2FCP (22), (23) to (36). Equation (36) converges to the third constant of motion (31) of the 2FCP as the time step $s^{(j+1)} - s^{(j)}$ approaches 0. Since the discrete 2FCP has three constants of motion $H_{\mathrm{d-c}}^{(j)}$, $I_{\mathrm{d}}^{(j)}$, $J_{\mathrm{d}}^{(j)}$, its trajectory is uniquely determined, as in the 2FCP.

5. Trajectories of discrete 2FCP

The 2FCP has various types of trajectories according to its initial condition. Cordani [2] classified these trajectories according to values of the constants of motion h_c and I. When the Hamiltonian h_c is negative, the motion of the moving particle is confined within a closed bounded region in the xy-plane. The region is determined by the values of h_c and I.

As we have seen in the previous section, the discrete 2FCP has the same two constants of motion $H_c^{(j)}$ and $I^{(j)}$ as the continuous 2FCP. Because of this property, the trajectories of the discrete 2FCP are restricted within the same region in the xy-plane as those of the 2FCP in the case $h_c < 0$. This is advantageous to long-time numerical simulations in the sense that the discrete 2FCP conserves a global characteristic of the original problem.

To begin with, we describe a classification of trajectories in the 2FCP. We assume $h_c < 0$. The 2FCP (8), (9) expressed by the elliptic coordinates $(\xi, \eta, p_\xi, p_\eta)$ are regarded as the Hamiltonian system with the time variable s and the following Hamiltonian:

$$K(\xi, \eta, p_\xi, p_\eta) \stackrel{\mathrm{def}}{=} K_\xi(\xi, p_\xi) + K_\eta(\eta, p_\eta), \tag{38}$$

where $K_\xi(\xi, p_\xi)$ and $K_\eta(\eta, p_\eta)$ are given in (6). Set γ as the value of K_ξ. Using the initial values $\xi(0)$ and $p_\xi(0)$ at $t = 0$, the following relationship is satisfied:

$$\gamma = \tfrac{1}{2}((\xi(0))^2 - 1)(p_\xi(0))^2 + \alpha\xi(0) - h_c(\xi(0))^2. \tag{39}$$

From (10), (6) reduces as follows:

$$\begin{aligned} \mathrm{d}\tau &= \frac{\mathrm{d}\xi}{\sqrt{(\xi^2 - 1)(h_c\xi^2 - \alpha\xi + \gamma)}}, \\ \mathrm{d}\tau &= -\frac{\mathrm{d}\eta}{\sqrt{(1 - \eta^2)(-h_c\eta^2 - \beta\eta - \gamma)}}, \end{aligned} \tag{40}$$

where $\tau (= \sqrt{2}s)$ is a new time parameter.

By integrating both sides, we can write ξ and η as elliptic functions of τ. The trajectories of 2FCP (8), (9) can be classified by the quartic polynomials under the radical sign. We set two quadratic polynomials, $M(\xi)$ and $Z(\eta)$, as

$$M(\xi) \stackrel{\mathrm{def}}{=} h_c\xi^2 - \alpha\xi + \gamma, \tag{41}$$

$$Z(\eta) \stackrel{\mathrm{def}}{=} h_c\eta^2 + \beta\eta + \gamma. \tag{42}$$

Note that $\alpha = -\alpha_1 - \alpha_2$, $\beta = \alpha_1 - \alpha_2$, $\alpha_1 \geqslant 0$ and $\alpha_2 \geqslant 0$ by definition. In (40) the quartic polynomial must be positive under the time evolution. Since $\xi \geqslant 1$ and $-1 \leqslant \eta \leqslant 1$ by definition (3), the relationship

$$M(\xi) \geqslant 0, \qquad Z(\eta) \leqslant 0 \tag{43}$$

Table 1. Classification of trajectories by h_c and γ.

Range of ξ	(A)	(A)	(A)	(A)	(B)	(B)	(B)	(B)
Range of η	(a)	(b)	(c)	(d)	(a)	(b)	(c)	(d)
Trajectory	I	I	–	–	II	II	III	IV

is satisfied. The discriminants of $M(\xi) = 0$ and $Z(\eta) = 0$ are $(\alpha_1 + \alpha_2)^2 - 4\gamma h_c$ and $(\alpha_1 - \alpha_2)^2 - 4\gamma h_c$, respectively. If $M(\xi)$ had complex roots, $Z(\eta)$ would also have complex roots. In this case, the condition (43) cannot be satisfied because the highest degree coefficients of $M(\xi)$ and $Z(\eta)$ have the same sign. Therefore, $M(\xi)$ always has two real roots. We write them as

$$\xi_+ \stackrel{\text{def}}{=} \frac{\alpha + \sqrt{\alpha^2 - 4\gamma h_c}}{2h_c}, \qquad \xi_- \stackrel{\text{def}}{=} \frac{\alpha - \sqrt{\alpha^2 - 4\gamma h_c}}{2h_c}. \tag{44}$$

As we assumed $h_c < 0$, ξ_- is greater than or equal to ξ_+. On the other hand, the root of $Z(\eta)$ can be complex. When $Z(\eta)$ has the real roots η_+ and η_-, they are

$$\eta_- \stackrel{\text{def}}{=} \frac{-\beta + \sqrt{\beta^2 - 4\gamma h_c}}{2h_c}, \qquad \eta_+ \stackrel{\text{def}}{=} \frac{-\beta - \sqrt{\beta^2 - 4\gamma h_c}}{2h_c} \tag{45}$$

and $\eta_- \geqslant \eta_+$. The variable ξ is in the range where $\xi \geqslant 1$ and $\xi_+ \leqslant \xi \leqslant \xi_-$. According to the values of ξ_+ and ξ_- there are two cases:

(A) $1 \leqslant \xi_+ \leqslant \xi \leqslant \xi_-$,
(B) $\xi_+ \leqslant 1 \leqslant \xi \leqslant \xi_-$.

Similarly, the variable η is in the range where $-1 \leqslant \eta \leqslant 1$ and '$\eta \leqslant \eta_+$ or $\eta \geqslant \eta_-$'. According to the values of η_+ and η_- there are four cases:

(a) $-1 \leqslant \eta \leqslant 1$ (complex roots),
(b) $-1 \leqslant \eta \leqslant 1 \leqslant \eta_+ \leqslant \eta_-$,
(c) $-1 \leqslant \eta \leqslant \eta_+ \leqslant 1 \leqslant \eta_-$,
(d) $-1 \leqslant \eta \leqslant \eta_+$ or $\eta_- \leqslant \eta \leqslant 1$.

The variable ξ indicates the sum of distances from the two fixed particles, and η indicates their difference. The curves $\xi = $ const. are ellipses with foci at $(1, 0)$ and $(-1, 0)$, and the curves $\eta = $ const. are hyperbolas with the same foci. $\xi \geqslant 1$ and $-1 \leqslant \eta \leqslant 1$ cover the whole xy-plane.

Table 1 shows the classification of the trajectories according to the ranges of ξ and η. Four types of trajectories, from case I to case I-.1emV, exist. The pairs (A)–(c) and (A)–(d) cannot be satisfied for any combination of h_c and γ.

Case I. In the areas (A)–(a) and (A)–(b), we have $\xi_+ \leqslant \xi \leqslant \xi_-$ and $-1 \leqslant \eta \leqslant 1$. The particle moves in the closed region bounded by the two ellipses $\xi = \xi_+$ and $\xi = \xi_-$.

Case II. In the areas (B)–(a) and (B)–(b), we have $1 \leqslant \xi \leqslant \xi_-$ and $-1 \leqslant \eta \leqslant 1$. The particle moves in the closed region bounded by the ellipse $\xi = \xi_-$.

Case III. In the areas (B)–(c), we have $1 \leqslant \xi \leqslant \xi_-$ and $-1 \leqslant \eta \leqslant \eta_+$. The particle moves in the closed region bounded by the ellipse $\xi = \xi_-$ and the hyperbola $\eta = \eta_+$.

Case IV. In the areas (B)–(d), we have $1 \leqslant \xi \leqslant \xi_-$ and '$-1 \leqslant \eta \leqslant \eta_+$ or $\eta_- \leqslant \eta \leqslant 1$'. The particle moves in the closed region bounded by the ellipse $\xi = \xi_-$ and one of the hyperbolas $\eta = \eta_+$ or $\eta = \eta_-$. Although the two possibilities exist, the initial condition determines which motion appears.

In the next place, we discuss the discrete 2FCP. We set the same initial discrete time $s^{(0)} = 0$ and initial condition $\left(x^{(0)}, y^{(0)}, p_x^{(0)}, p_y^{(0)}\right) = (x(0), y(0), p_x(0), p_y(0))$ as the 2FCP

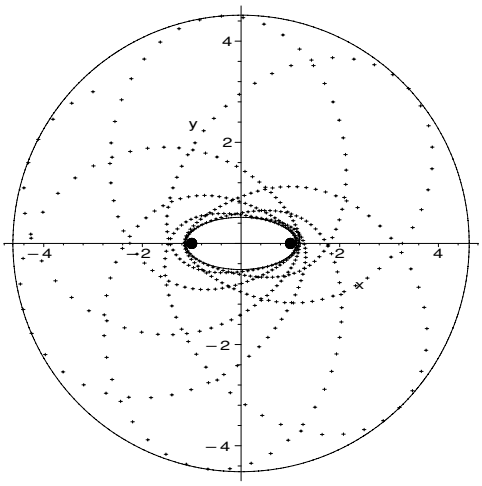

Figure 1. Case I (the ellipses are $\xi = \xi_+, \xi_-$).

has. We define the discrete canonical variables $\xi^{(j)}$, $\eta^{(j)}$, $p_\xi^{(j)}$ and $p_\eta^{(j)}$ by the following relationship:

$$\xi^{(j)} = \cosh u^{(j)}, \qquad \eta^{(j)} = \cos v^{(j)}, \qquad p_\xi^{(j)} = \frac{p_u^{(j)}}{\sinh u^{(j)}}, \qquad p_\eta(j) = -\frac{p_v^{(j)}}{\sin v^{(j)}}, \tag{46}$$

which parallels the canonical transformation (11) of the 2FCP. Naturally, $\xi^{(j)} \geqslant 1$, $-1 \leqslant \eta^{(j)} \leqslant 1$, $j = 0, 1, 2, \ldots$. The discrete 2FCP preserves the same constants of motion $K_u\big(u^{(j)}, p_u^{(j)}\big)$ and $K_v\big(v^{(j)}, p_v^{(j)}\big)$ as the 2FCP. Set γ as the value of $K_u\big(u^{(j)}, p_u^{(j)}\big)$. The following identities are satisfied:

$$\big(p_\xi^{(j)}\big)^2 = 2\frac{h_c(\xi^{(j)})^2 - \alpha\xi^{(j)} + \gamma}{(\xi^{(j)})^2 - 1} \geqslant 0, \tag{47}$$

$$\big(p_\eta^{(j)}\big)^2 = -2\frac{h_c(\eta^{(j)})^2 + \beta\eta^{(j)} + \gamma}{1 - (\eta^{(j)})^2} \geqslant 0. \tag{48}$$

As both $(\xi^{(j)})^2 - 1$ and $1 - (\eta^{(j)})^2$ are positive, the two inequalities $M(\xi^{(j)}) \geqslant 0$ and $Z(\eta^{(j)}) \leqslant 0$ are given. Using these inequalities, we get the same classification of the trajectories of the discrete 2FCP as those of the 2FCP.

The above discussion shows that, when $h_c < 0$, the trajectories of the discrete 2FCP are restricted within the same region as those of the 2FCP. In the case where $h_c \geqslant 0$, we can study the time evolution of the discrete 2FCP in a similar way.

We get the trajectory of the discrete 2FCP in every case from I to IV. Figures 1–4 give the trajectories in the xy-plane. In these figures the solid curves are ellipses or hyperbolas that define the region in which the moving particle is confined. Two black circles indicate the position of the fixed particles. We give $\mu = 0.6$ and $s^{(j+1)} - s^{(j)} = 0.05$, $j = 0, 1, \ldots$. The number of iterations is $N = 500$. In each figure we set the initial condition as follows:

Figure 1: case I $\big(x^{(0)}, y^{(0)}, p_x^{(0)}, p_y^{(0)}\big) = (-3.0, 3.0, -0.5, -0.2)$,
Figure 2: case II $\big(x^{(0)}, y^{(0)}, p_x^{(0)}, p_y^{(0)}\big) = (0.0, 1.0, 0.5, 0.0)$,

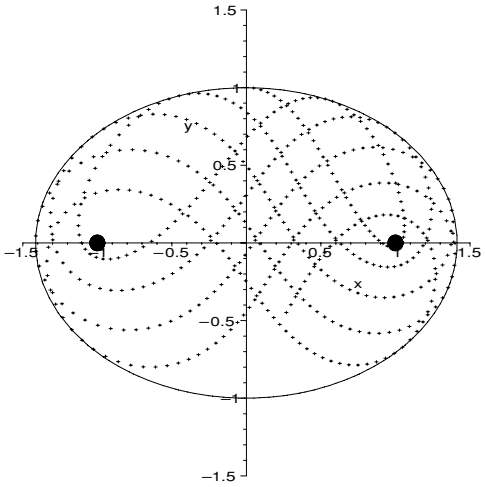

Figure 2. Case II (the ellipse is $\xi = \xi_-$).

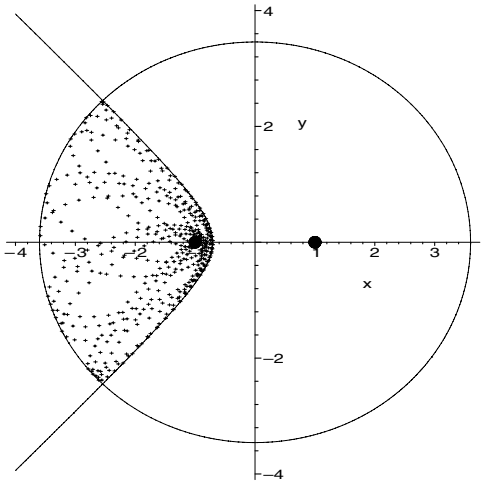

Figure 3. Case III (the ellipse is $\xi = \xi_-$ and the hyperbola is $\eta = \eta_-$).

Figure 3: case III $\left(x^{(0)}, y^{(0)}, p_x^{(0)}, p_y^{(0)}\right) = (-3.0, 1.0, 0.5, 0.1)$,
Figure 4: case IV $\left(x^{(0)}, y^{(0)}, p_x^{(0)}, p_y^{(0)}\right) = (-1.0, 1.0, -0.5, 0.0)$.

We observe that the trajectory of the discrete 2FCP lies within the regions determined by the values h_c and γ.

Since the discrete system (18) has no singularities, the values of $u^{(j)}$ and $p_u^{(j)}$ do not overflow. However, the discrete fictitious time step $s^{(j+1)} - s^{(j)}$ includes a singularity because (21) is rewritten as

$$s^{(j+1)} - s^{(j)} = \frac{t^{(j+1)} - t^{(j)}}{(\cosh^2 u^{(j)} - \cos^2 v^{(j)})} = \frac{t^{(j+1)} - t^{(j)}}{r_1 r_2}. \tag{49}$$

If $t^{(j+1)} - t^{(j)}$ is constant, $s^{(j+1)} - s^{(j)}$ becomes greater as the moving particle approaches a fixed particle. This increases discretization error. Actually, in cases II, III and IV, the distance

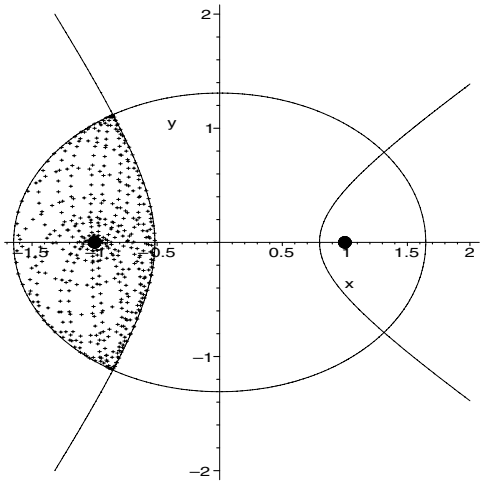

Figure 4. Case IV (the ellipse is $\xi = \xi_-$ and the hyperbolas are $\eta = \eta_+, \eta_-$).

between the moving and the fixed particles can become infinitesimally small [18]. This causes an overflow of the value $s^{(j+1)} - s^{(j)}$ and then a loss of accuracy. By setting $s^{(j+1)} - s^{(j)}$ constant, we can avoid such overflow near the fixed particles. This introduces a variable time step $t^{(j+1)} - t^{(j)}$ for the discrete 2FCP (23), (22).

6. Numerical results

In this section we compare the discrete 2FCP (18) and (20) with a symplectic integrator (cf [5, 16]). Symplectic integrators are generally used to simulate Hamiltonian systems numerically. The symplectic integrator of order 1 is applied to the Hamiltonian system (14) and (15). Then the following discrete system is given:

$$\begin{aligned} &\Delta_{+s} u^{(j)} = p_u^{(j)}, \qquad && \Delta_{+s} p_u^{(j)} = -\alpha \sinh u^{(j+1)} - 2A \cosh u^{(j+1)} \sinh u^{(j+1)}, \\ &\Delta_{+s} v^{(j)} = p_v^{(j)}, \qquad && \Delta_{+s} p_v^{(j)} = \beta \sin v^{(j+1)} - 2A \cos v^{(j+1)} \sin v^{(j+1)}, \qquad j = 0, 1, \ldots. \end{aligned} \tag{50}$$

Here the relationship between the fictitious discrete time $s^{(j)}$ and the discrete time $t^{(j)}$ is given by (21). We set $s^{(j+1)} - s^{(j)}$ constant for every $j = 0, 1, \ldots$. The discrete system (50) is an explicit scheme, and is regarded as a discrete analogue of the 2FCP.

Although symplectic integrators do not conserve the Hamiltonian, they are known to conserve an approximate Hamiltonian [5, 16]. The system (50) keeps the values of the following $\tilde{K}_u^{(j)}$, $\tilde{K}_v^{(j)}$:

$$\begin{aligned} \tilde{K}_u^{(j)} &= K_u^{(j)} + \frac{\delta}{2} \left(\frac{\partial K_u}{\partial u} \right)^{(j)} \left(\frac{\partial K_u}{\partial p_u} \right)^{(j)} + O(\delta^2) \\ &= K_u^{(j)} + \frac{\delta p_u^{(j)}}{2} (\alpha \sinh u^{(j)} + 2A \cosh u^{(j)} \sinh u^{(j)}) + O(\delta^2), \\ \tilde{K}_v^{(j)} &= K_v^{(j)} + \frac{\delta}{2} \left(\frac{\partial K_v}{\partial v} \right)^{(j)} \left(\frac{\partial K_v}{\partial p_v} \right)^{(j)} + O(\delta^2) \end{aligned} \tag{51}$$

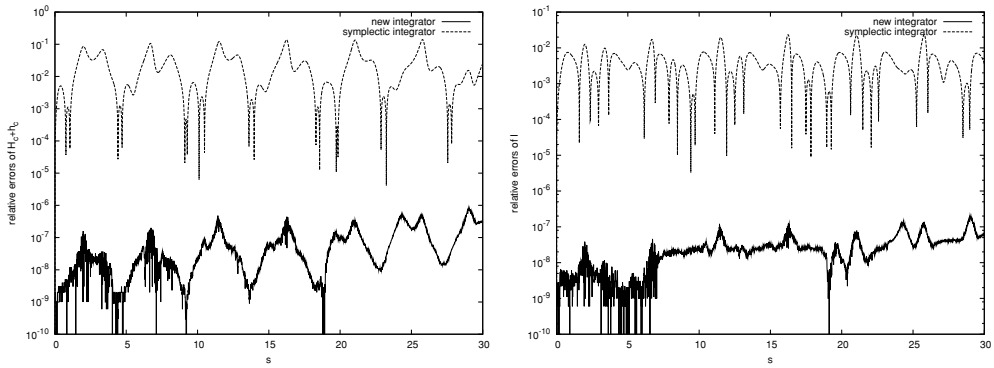

Figure 5. Relative errors of $H_c + h_c$ and I.

$$= K_v^{(j)} + \frac{\delta p_v^{(j)}}{2}(-\beta \sin v^{(j)} + 2A \cos v^{(j)} \sin v^{(j)}) + O(\delta^2),$$

$$\delta \stackrel{\text{def}}{=} s^{(j+1)} - s^{(j)}, \qquad j = 0, 1, 2, \ldots, \tag{52}$$

where $\tilde{K}_u^{(j)}$ and $\tilde{K}_v^{(j)}$ are discrete analogues of K_u and K_v, respectively. Equation (27) shows that the constant $-K_u$ is the very constant I of the 2FCP. Consequently, $-\tilde{K}_u^{(j)}$ is seen as the discrete analogue $\tilde{I}^{(j)}$ which goes to the constant I of the 2FCP as $s^{(j+1)} - s^{(j)} \to 0$. Moreover, the Hamiltonian H_c of 2FCP is expressed as a function of K_u and K_v in (26). We define $\tilde{\mathcal{H}}^{(j)}$ as

$$\tilde{\mathcal{H}}^{(j)} \stackrel{\text{def}}{=} \frac{\tilde{K}_u^{(j)} + \tilde{K}_v^{(j)}}{\cosh^2 u^{(j)} - \cos^2 v^{(j)}}. \tag{53}$$

Here $\tilde{\mathcal{H}}^{(j)}$ is a discrete analogue of H_c of the 2FCP. As the time step $s^{(j+1)} - s^{(j)}$ is constant and the following relationship holds

$$\frac{\tilde{K}_u^{(j)} + \tilde{K}_v^{(j)}}{s^{(j+1)} - s^{(j)}} = \tilde{\mathcal{H}}^{(j)}(t^{(j+1)} - t^{(j)}), \tag{54}$$

$\tilde{\mathcal{H}}^{(j)}(t^{(j+1)} - t^{(j)})$ leads to a constant. So the symplectic integrator has a constant of motion $\tilde{\mathcal{H}}^{(j)}(t^{(j+1)} - t^{(j)})$, which is a discrete analogue of $H\mathrm{d}t$ of the 2FCP.

Figure 5 shows the relative errors of $H_c + h_c$ and I given by the discrete 2FCP and the symplectic integrator, respectively. The solid lines indicate the discrete 2FCP, and the dotted lines indicate the symplectic integrator. We set the initial condition as $\left(x^{(0)}, y^{(0)}, p_x^{(0)}, p_y^{(0)}\right) = (-3.0, 3.0, -0.5, -0.2)$ and $\mu = 0.6$, which corresponds to case I of the previous section. We put the constant time step $\delta \stackrel{\text{def}}{=} s^{(j+1)} - s^{(j)} = 0.01$ and the number of iteration $N = 3000$. We use Maple to implement floating point operations of the numerical schemes. We set ten significant digits in the decimal system. The greatest possible round error caused by one floating point operation is $\epsilon \stackrel{\text{def}}{=} \frac{1}{2} \times 10^{-9}$. The discrete 2FCP gives the relative error of $H_c + h_c$ and I smaller than $3000\epsilon = \frac{3}{2} \times 10^{-6}$ after 3000 steps. This confirms that the discrete 2FCP conserves H_c and I. On the other hand, the symplectic integrator does not exactly conserve H_c and I.

Figure 6 presents the trajectory given by the symplectic integrator (50) in the xy-plane. We set the same initial condition $(x^{(0)}, y^{(0)}, p_x^{(0)}, p_y^{(0)}) = (-3.0, 3.0, -0.5, -0.2)$, $\mu = 0.6$, $s^{(j+1)} - s^{(j)} = 0.05$ and $N = 500$ as figure 1 in the previous section. Since the symplectic

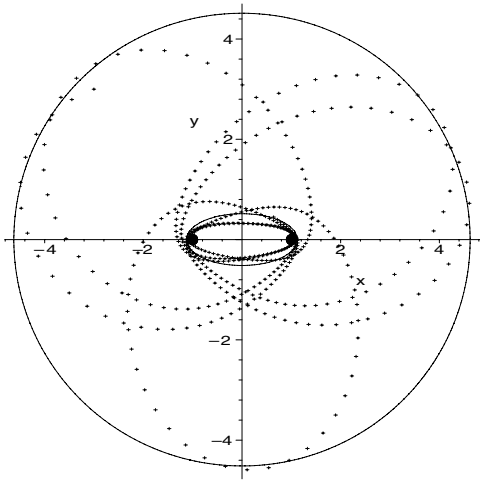

Figure 6. Time evolution by the symplectic integrator (the ellipses are $\xi = \xi_+, \xi_-$).

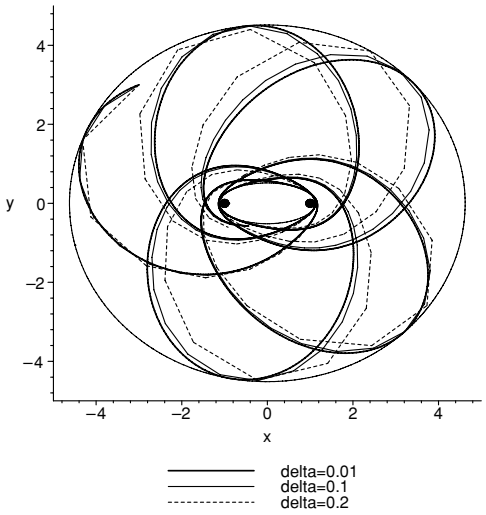

Figure 7. Time evolution by a new integrator (step sizes $\delta = 0.01, 0.1, 0.2$).

integrator does not conserve H_c and I, the trajectory does not stay in the bounded region framed by the two solid-line ellipses.

Figure 7 presents the trajectories of the discrete 2FCP with different step sizes δ. The bold, solid and dotted lines are the trajectories with the time step $\delta = 0.01, 0.1$ and 0.2, respectively. The time interval in the separated system $\delta \times N = 1000$ is kept constant. The case $\delta = 0.01$ is closest to the trajectory of the 2FCP. As the time step-size becomes greater, the deviation from the trajectory of 2FCP increases. This drift seems to stem from a characteristic of the discrete 2FCP that it conserves only two constants of motion H_c and I while the 2FCP has three constants of motion H_c, I and J. However, the trajectories of the discrete 2FCP stay in the closed region bounded by two ellipses.

7. Conclusion

In this paper we have proposed a numerical integrator for the 2FCP which conserves two constants of motion. The canonical variables in [18] are introduced to separate the variables, and then the singularities are removed. Then we discretize the system by applying the energy-preserving method to each part of the separated Hamiltonian system. As a result, the discrete 2FCP has two constants of motion which have the same form as those of the continuous system. It is also shown that the discrete 2FCP has an additional constant of motion. This is a discrete analogue of the 2FCP's third constant of motion which has an integral form.

Since the discrete 2FCP conserves two constants of motion of the continuous system, the trajectories of the discrete 2FCP are confined in the same closed bounded region as those of the 2FCP. As a result, the discrete and continuous 2FCP can be classified in the same way. This is advantageous to a long-time numerical simulation in the sense that the discrete 2FCP conserves a global characteristic of the 2FCP. We have conducted a numerical experiment and have compared the result with that of a symplectic integrator. Time evolution by the symplectic integrator shows drift from the closed region of the continuous 2FCP. While this drift can be reduced by introducing higher order symplectic integrators, the discrete 2FCP is still advantageous when an initial condition is set close to a boundary of two qualitatively different orbits.

In the last few decades, geometric integration of dynamical systems have become popular and various properties such as first integrals, symplecticness, reversibility, symmetry or group structure are utilized to develop novel numerical methods. Conserving several properties simultaneously is usually costly, or sometimes even impossible. Therefore, one has to choose an appropriate method to meet his needs. This paper concentrates on the constants of motion of the two-fixed-centres problem, and the proposed method conserves unique geometric property that the continuous system has.

References

[1] Contopoulos G and Papadaki H 1993 Newtonian and relativistic periodic orbits around two fixed black holes *Celest. Mech. Dyn. Astron.* **55** 47–85

[2] Cordani B 2003 *The Kepler Problem* (Basel: Birkhäuser)

[3] Greenspan D 1974 *Discrete Numerical Method in Physics and Engineering* (New York: Academic)

[4] Greenspan D 2004 *N-body Problems and Models* (Hackensack, NJ: World Scientific)

[5] Hairer E 1994 Backward analysis of numerical integration and symplectic methods *Ann. Numer. Math.* **1** 107–32

[6] Hairer E, Lubich C and Wanner G 2002 *Geometric Numerical Integration: Structure-Preserving Algorithms for Ordinary Differential Equations* (Berlin: Springer)

[7] Hirota R 2003 *Lectures on Difference Equations* (Tokyo: Saiensusha) (in Japanese)

[8] Itoh T and Abe K 1988 Hamiltonian-conserving discrete canonical equations based on variational difference quotients *J. Comp. Phys.* **77** 85–102

[9] Leimkuhler B and Reich S 2004 *Simulating Hamiltonian Dynamics* (Cambridge: Cambridge University Press)

[10] Marsden J E and West M 2001 Discrete mechanics and variational integrators *Acta Numer.* **10** 357–514

[11] McLachlan R I and Quispel R G W 2006 Geometric integrators for ODEs *J. Phys. A: Math. Gen.* **39** 5251–85

[12] Minesaki Y and Nakamura Y 2002 A new discretization of the Kepler motion which conserves the Runge–Lenz vector *Phys. Lett.* A **306** 127–33

[13] Minesaki Y and Nakamura Y 2004 A new conservative numerical integration algorithm for the three-dimensional Kepler motion based on the Kustaanheimo–Steifel regularization theory *Phys. Lett.* A **324** 282–92

[14] Minesaki Y and Nakamura Y 2006 New numerical integrator for the Stäckel system conserving the same number of constants of motions as the degree of freedom *J. Phys. A: Math. Gen.* **39** 9453–76

[15] Perelomov A M 1990 *Integrable Systems of Classical Mechanics and Lie Algebras* vol 1 (Basel: Birkhäuser)

[16] Sanz-Serna J M and Calvo M P 1994 *Numerical Hamiltonian Problems* (London: Chapman and Hall)

[17] Tsiganov A V 1999 Duality between integrable Stäckel systems *J. Phys. A: Math. Gen.* **32** 7965–82

[18] Varvoglis H, Vozikis Ch and Wodnar W 2004 The two fixed centers: an exceptional integrable system *Celest. Mech. Dyn. Astron.* **89** 343–56

[19] Wendlandt J M and Marsden J E 1997 Mechanical integrators derived from a discrete variational principle *Physica* D **106** 223–46

[20] Yoshida H 1993 Recent progress in the theory and application of symplectic integrators *Celest. Mech. Dyn. Astron.* **56** 27–43